Optimization of host cell-compatible, antimicrobial peptides effective against biofilms and clinical isolates of drug-resistant bacteria.

[1]Ghimire, J., [2]Hart, J.R., [3]Soldano, A, [4]Chen, C., [1]Guha S., [2]Hoffmann, J., [2]Hall, K., [1]Sun, L., [1]Nelson, B.J., [4]Lu, TK, [5]Kolls, J.K., [3]Rivera, M., [2]Morici, LA., and [1]Wimley, WC.

[1]Tulane University School of Medicine, Department of Biochemistry and Molecular Biology. New Orleans, LA

[2]Tulane University School of Medicine, Department of Microbiology and Immunology, New Orleans, LA

[3]Louisiana State University, Department of Chemistry, Baton Rouge, LA

[4]Synthetic Biology Group, Research Laboratory of Electronics, Massachusetts Institute of Technology (MIT), Cambridge, MA

[5]Tulane University School of Medicine, Department of Medicine, New Orleans, LA

Abstract

Here, we describe the synthetic molecular evolution of a family of host-compatible antimicrobial peptides (AMP) designed for the treatment of wounds infected with drug-resistant, biofilm forming bacteria. The peptides tested are variants of an evolved AMP called D-CONGA, which has excellent antimicrobial activities *in vitro* and *in vivo*. In this generation of rational D-CONGA variants, we tested multiple sequence-function hypotheses that had not been tested in previous generations. Many of the peptide variants tested have lower antibacterial activity against Gram-positive and Gram-negative pathogens, especially those that have altered hydrophobicity, secondary structure potential, or spatial distribution of charged and hydrophobic residues. Thus, D-CONGA is generally well tuned for good antimicrobial activity. However, we identified one variant, D-CONGA-Q7, with a polar glutamine inserted into the middle of the sequence, that has higher activity against both planktonic and biofilm-forming bacteria and lower cytotoxicity against human fibroblasts. Against clinical isolates of *K. pneumoniae*, innate resistance to D-CONGA was surprisingly common despite a lack of inducible resistance in *P. aeruginosa* reported in our previous work. Yet, these same isolates are susceptible to D-CONGA-Q7. Additional mechanistic work will be required to understand why D-CONGA-Q7 is less prone to innate resistance in Gram-negative bacteria. In the spirit of synthetic molecular evolution, the discovery of D-CONGA-Q7 achieved a critical gain-of-function, and has provided a significantly better template sequence for the next generation of synthetic evolution.

Introduction

Membrane permeabilizing antimicrobial peptides have long been recognized as a promising, but mostly unfulfilled, chemotype in the development of new drugs to treat drug-resistant bacterial infections[1-3]. Thousands of AMPs have been described in the literature[4], many with potent, broad-spectrum antimicrobial activity against bacterial pathogens *in vitro*. However, due to multiple known impediments to AMP activity *in vivo*, [5-7] few have reached late-stage clinical trials. Among the many known AMPs, only polymyxin (colistin) and daptomycin, both naturally occurring lipopeptides, have been approved for use in humans in the US and Europe.

An AMP that is useful, for example in wound treatment, must simultaneously be optimized for antimicrobial activity against multiple microbes but also for lack of impediments, including host cell, tissue, and protein binding, as well as cytotoxicity, proteolytic degradation, and low solubility. These various activities are complex, multifactorial, and interdependent such that simultaneous rational optimization is not possible. AMP activity against bacteria, alone, is so complex and poorly understood that it defies easy explanation, except in the very broadest terms. It depends, ultimately, on cytoplasmic membrane disruption[1-2], which requires "interfacial activity"[8]. Interfacial activity is contingent upon strong membrane binding coupled with imperfect amphipathicity, which disrupts lipid organization in bilayers. However, accurately predicting which sequences will be effective at bacterial membrane permeabilization or foreseeing how to improve activity or reduce impediments has never been possible.

Common impediments to AMP activity *in vivo* include binding to host cells and tissues[7], proteolytic degradation[6], residual toxicity, and low solubility. Rationally reducing these unwanted activities, while also optimizing antimicrobial activity against multiple species of bacteria has not been possible because the fundamental sequence-structure-function relationships of these various biological activities are not understood well enough for quantitative sequence-structure activity relationships (QSAR) to be described. Deconvolution of the interdependent contributions to activity, toxicity, solubility, and host-cell binding is not possible. Thus, most AMP discovery in the literature is the result of trial and error, based on known sequences, which can be natural or synthetic. We have embraced the spirit of trial and error to efficiently work towards solving the problem of identifying new "host-compatible" AMPs[5], lacking the known impediments, by using synthetic molecular evolution (SME)[5]. SME is the orthogonal screening of multiple, iterative generations of small libraries of 5-30,000 members under increasingly clinically relevant

conditions. SME enables us to test thousands of closely related sequences to identify AMPs with the best broad-spectrum antimicrobial activity, while also down-selecting for the known impediments. Our libraries are each designed to test the contribution of a small number of rational variations. After a generation of screening to identify gain-of-function variants, we have found it useful to carry out small-scale semi-rational variation to test other hypotheses that had not been tested previously in libraries. Such cycles of library screening, followed by rational trial and error, have led to an improved understanding of sequence-function relationships, which results in more intelligent, next-generation AMP library design. This approach has led to continuously improved combinations of desirable properties.

Here, we describe a new AMP with exceptional activities that has resulted from two generations of library screening plus two rounds of rational variation. See **Fig. 1** for a history. In the first generation, we screened a *de novo* designed peptide library for members that permeabilize bacteria-like lipid vesicles[9-10]. In parallel, we screened the same library for members that have broad spectrum antibacterial activity in simple, defined media[11]. These two screens enabled the identification of two distinct families of potent, broad-spectrum AMPs from a single library. We subsequently showed that these first-generation AMPs, like most others, have a list of impediments to *in vivo* activity: i) they lose activity in the presence of concentrated host cells; ii) they have relatively low solubility, and iii) they have some residual toxicity[11], and iv) they are rapidly degraded by serum endopeptidases[6]. We thus designed and synthesized an iterative second-generation library that we screened for multi-organism, sterilizing activity <u>in the presence of concentrated human erythrocytes[5],</u> to downselect against host cell binding. We also downselected against cytotoxicity by measuring hemolysis in parallel, and against insoluble peptides, by pre-incubating in saline solution prior to assays. Having shown that L- and D-amino acid enantiomers of these AMPs have identical activities[5, 7, 11], we tested the peptides using protease-resistant D-amino acid peptides to eliminate proteolytic degradation by serum exopeptidases. This second-generation screen led to the discovery of the so-called D-DBS (D-amino acid <u>D</u>ouble <u>B</u>roth <u>S</u>terilization) peptides, which have broad spectrum sterilizing activity against a panel of Gram-positive and Gram-negative pathogens[5], **Fig. 1**. Importantly, the DBS peptides are fully active in the presence of concentrated host cells and have high solubility (>1 mM) in physiological saline solution. We created a consensus sequence and subsequently obtained some improvement by the removal of two invariant glycines[5]. This lead peptide D-CONGA (<u>D</u>-amino acid <u>CON</u>sensus with

Glycine Absent), which has been described in detail[5], is highly soluble, highly stable, and has moderately low cytotoxicity, while also having broad-spectrum, antibacterial, and anti-biofilm activity *in vitro* and *in vivo*, even in the presence of host cells, serum proteins, and tissue[5].

In the current work, we subjected the lead peptide D-CONGA to a broad series of rational variations to catalog important factors for its overall characteristics as an antibiotic. We find that the properties of D-CONGA are mostly well-tuned. Most variations to its sequence either decrease antimicrobial activity and toxicity, or have no effect. However, we identified a new variant, called D-CONGA-Q7, with a polar glutamine inserted between the cationic and hydrophobic segments of the peptide, that has significantly improved antibiotic activity, significantly better anti-biofilm activity, and lower residual toxicity compared to D-CONGA. Perhaps most importantly, the newly discovered peptide, D-CONGA-Q7 has significantly improved activity against clinical isolates of drug-resistant bacteria, including isolates of the problematic Gram-negative species *K. pneumoniae*, some of which are resistant to the parent peptide D-CONGA.

Methods

Synthesis of the peptide variants

All peptides used in this study were synthesized using solid-phase FMOC chemistry and purified to >95% using high-performance liquid chromatography (HPLC) either in the laboratory or by Bio-synthesis Inc. In all cases, peptide identity was confirmed through MALDI mass spectrometry. Unless otherwise stated, all solutions were prepared by dissolving lyophilized peptide or antibiotic powders in 0.025% (v/v) acetic acid in water. Peptide concentrations were determined by optical absorbance at 280 nm.

Bacterial strains and growth conditions

E. coli (ATCC 25922), *S. aureus* (ATCC 25923), and *K. pneumoniae subsp. pneumoniae* (ATCC 13883), were used for the comparison of MIC values in this study. Subcultures, prepared by inoculating 25 mL of fresh tryptic soy broth (TSB) with 200 µL of an overnight culture, were grown to log phase (OD600 = 0.3−0.6), after which cell counts were determined by measuring the OD600 (1.0 = $5x10^8$ CFU/mL for *E. coli*, $4x10^8$ CFU/mL for *K. pneumoniae*, $4x10^8$ CFU/mL for *P. aeruginosa*, $1.5x10^8$ CFU/mL for *S. aureus*). Bacterial cells were diluted to appropriate concentrations in TSB. We used the following clinical bacterial isolates of *Klebsiella pneumoniae* in this study: Strains KP6, KP46, NDM-1, KP396, and KP398 have been previously described[12]. ST58 strains C2, C3, and I2 are also described[13]. The alternate KP isolate is ATCC 33495. MRSA,

multidrug resistant *Staphylococcus aureus* strain, is SAP400, a USA400 strain of community acquired MRSA. AB, *Acinetobacter baumanii*, is a pan drug resistant (PDR) strain isolated in the Tulane Hospital in 2015. The second independent set of *K. pneumoniae* isolates are previously described[14-15].

The susceptibility of biofilm-embedded *P. aeruginosa* cells to the antimicrobial peptides was studied as reported previously[16] using a *P. aeruginosa* PAO1 strain expressing enhanced yellow fluorescent protein (EYFP)[17]. The EYFP-expressing *P. aeruginosa* strain was routinely grown in *Pseudomonas* Isolation (PI) media (20 g/L peptone, 0.3 g/L, $MgCl_2 \cdot 6H_2O$, 10 g/L, K_2SO_4, 25 mg/L irgasan, and 20 mL/L glycerol, pH 7.0). Pellicle biofilms were treated in AB minimal media[18] with trace metals [0.15 μM $(NH_4)_2MoO_4$, 3 μM $CuSO_4$, 2 μM $Co(NO_3)_2$, 9.4 μM $Na_2B_4O_7$, and 7.6 μM $ZnSO_4$], 3 mM glucose and 15 μM Fe. The media used for the treatment included a final concentration of 0.0025% acetic acid. Iron supplementation was carried out by addition of a small volume of filter-sterilized 10 mM $(NH_4)_2Fe(SO_4)_2$ (pH ~2.0) solution. The antibiotic colistin was used at concentrations equivalent to 12.5× and 25× the reported MIC = 1 μg/mL = 0.79 μM[19]. Antimicrobial peptides stock solutions in 0.025% acetic acid were freshly prepared, stored at 4 °C ,and diluted in the AB challenge media used to treat biofilms at the concentrations specified in the figure captions.

Human red blood cells.

Human O+ erythrocytes were obtained from Interstate Blood Bank, Inc. Red blood cells were subjected to four or more cycles of centrifugation at 1000xg with resuspension in fresh PBS. Following the final wash step, the supernatant was clear and colorless. RBC concentration was determined using a standard hemocytometer.

Broth dilution assay

Antimicrobial peptides and conventional antibiotics were prepared at 5-times the final concentration needed in 0.025% acetic acid. The antibiotics were serially diluted by a factor of 2:3 horizontally across 96-well plates from Corning, 25 μL per well. One column was reserved for controls. For the assays performed in the presence of RBC, type O+ human RBCs at 0 or 2.5×10^9 cells/mL were added in 50 μL aliquots to all wells. Following a 30-minute incubation, 50 μL of TSB, inoculated with 5×10^5 CFU/mL, was added to all wells, and plates were incubated overnight at 37 °C. Following overnight incubation at 37° C, the OD600 was measured (values of less than 0.1 were considered sterilized). To assess bacterial growth in the assays with RBC, the OD600

was measured after a second day inoculation with 10 μL of solution from the original plate added to 100 μL of sterile TSB followed by overnight incubation.

***Hemolysis* assay**

Peptide was serially diluted in PBS starting at a concentration of 100 μM. The final volume of peptide in each well was 50 μL. To each well, 50 μL of RBCs in PBS at $2x10^8$ cells/mL was added. As a positive lysis control, 1% triton was used. The mixtures were incubated at 37°C for 1 hour, after which they were centrifuged at 1000g for 5 minutes. After centrifugation, 10 μL of supernatant was transferred to 90 μL of DI H_2O in a fresh 96-well plate. The absorbance of released hemoglobin at 410 nm was recorded, and the fractional hemolysis was calculated based on the 100% and 0% lysis controls.

SYTOX Green Cytotoxicity Assay.

WI-38 human fibroblast cells were grown to confluency in T-75 flasks in complete DMEM (10% FBS). The day before cytotoxicity experiments, the 10,000 cells/well cells were plated in a 96-well tissue-culture plate. The next day, in a separate 96-well plate, peptides were serially diluted in serum-free DMEM with 0.1% SYTOX green starting at concentrations of 100 μM and 50 μM, followed by 2:3 serial dilutions horizontally across the plate. To perform the cytotoxicity assay, media was removed from the wells and replaced with the peptide solutions. No peptide and 20 μM Melp5, a highly lytic peptide, were used as negative and positive control, respectively. The plate was read for SYTOX fluorescence every 5 minutes for an hour with an excitation wavelength of 504 nm and an emission wavelength of 523 nm. Percent cytotoxicity was calculated at 60 min using the 100% and 0% lysis controls.

Biofilm assays

These experiments were carried out as described previously[16-17]. In brief: Starter cultures (5 mL PI media supplemented with 10 μM Fe) were grown (14 h) from a single colony shaking (220 rpm) at 37 °C. To grow the pellicle biofilms, starter cultures were diluted to OD_{600} = 0.001 in 4 mL PI media supplemented with 20 μM Fe, placed in 35 x 10 mm petri dishes and incubated statically at 30 ºC for 48 h. The pellicles were harvested using circular (1.5 cm diameter) glass coverslips by gently allowing the surface of a coverslip to contact the biofilm at the air-liquid interface. The pellicle-adhered coverslip was washed in PBS and then deposited on top of 1.5 mL AB challenge media contained in a well of a 12-well microplate, with the pellicle exposed to the challenge media and incubated statically at 30 °C for 24 h. The biofilms were then washed by transferring the

coverslip-adhered pellicles (biofilm facing down) into 35 x 10 mm petri dishes containing 4 mL PBS, and incubating for 5 min. To release cells from the biofilm and break the extracellular matrix, the coverslip-adhered pellicles were placed in 50 mL conical tubes containing a 2 mL suspension of zirconia beads (0.1 mm diameter, BioSpec Products), 10 mL PBS, 0.2 µg/mL alginate lyase and 0.2 µg/mL DNase, incubated at room temperature for 15 min, and then vortexed for 4 min. After sedimentation of the zirconia beads, a 100 µL aliquot was used for serial dilution and plating on PIA plates for enumeration of viable cells (CFU/mL).

Confocal laser scanning microscopy of biofilms.

These experiments were conducted as reported previously (**1**). In brief: Pellicles were washed in PBS and then stained with Sytox Red by placing the coverslip-adhered pellicles in 1 mL of PBS containing 2.5 nM of the fluorescent dye for 15 min. Excess dye was washed with PBS, the coverslip was mounted on a glass slide using 5 µL SlowFade (Invitrogen Life Technologies) and the edges sealed with fingernail polish. The biofilms were imaged with the aid of a Leica TCS SP8 confocal microscope (Leica Microsystems, Germany) using a HC PL apo CS2 63×/1.4 oil objective. For detecting the EYFP fluorescence the laser line was set at 506 nm and the emission range to 520−610 nm. Sytox Red fluorescence was detected with excitation at 631 nm and emission range 637−779 nm. Image stacks were acquired with a *z*-step size of 0.3 µm at randomly chosen positions and the Leica Application Suite X (LAS-X) software was used for image stack processing. Quantitative analysis was performed by determination of pellicle biomass using COMSTAT[20-21] and the Otsu method of automatic thresholding[22].

Statistical Analysis. One-way ANOVA followed by Tukey's multiple *post hoc* test was used to determine the statistical significance between the means and standard deviation of untreated *vs* treated with antimicrobial agents, with the aid of SigmaPlot (Systat Software, Inc. CA).

Wound infection model

All animal studies strictly adhered to protocol 131 which was approved by Tulane University Institutional Animal Care and Use Committee. Female CD1 mice at 8-12 weeks of age were anesthetized via intraperitoneal injection of ketamine and xylazine at doses of 90 mg/kg and 10 mg/kg, respectively. Their dorsal surface was depilated using an electric razor and scrubbed with a chlorhexidine solution. A full thickness biopsy wound was generated using a 5 mm biopsy punch (Integra). To function as a splint for the wound, a silicon (Invitrogen) ring 0.5 mm thick with an outer diameter of 10mm and a hole with a 5mm diameter was placed over the wound and held to

the skin with a surgical adhesive. The entire silicon ring was then covered with Tegaderm (3M), and further adhered using 4-0 braided silk interrupted sutures (Ethicon). Mice were given 0.05 mg/kg buprenorphine immediately following surgery as well as daily for the next two days to alleviate pain from the procedure. Wound beds were infected by penetrating the Tegaderm with an insulin syringe and injecting $1x10^4$ colony forming units (CFUs) of *P. aeruginosa* (PAO1) or MRSA suspended in 10 µL sterile PBS directly onto the wound bed. All bacteria used were pelleted during early exponential growth phase prior to infection. Four hours after infection mice were topically treated with 75 µg D-CONGA-Q7 in 0.025% acetic acid or vehicle only in a 20µL volume, by penetrating the Tegaderm with an insulin syringe and injecting the treatment directly on the wound bed. Treatment was administered every 8 hours for the first 5 days of infection. Mice were imaged daily for two weeks using the *in vivo* imaging system (IVIS)-XMRS (PerkinElmer), and bioluminescence generated from the bacteria was quantified in values of radiance (photons/sec). Weight, activity, posture, coat condition and wound condition were monitored each day throughout the duration of the experiment to ensure the wellbeing of each mouse.

Scanning electron microscopy

Tegaderm dressings were removed from wounds of each mouse on Day 3 after infection. Tegaderm were washed with PBS and attached to hydroxyapatite discs placed horizontally in 24-well microtiter plates. Following this, the tegaderm was fixed by placing the discs in 200 µl of 2.5% glutaraldehyde. The fixed samples were dehydrated using increasing concentrations of ethanol and then desiccated with CO_2 critical point drying. The samples were carbon coated and subjected to scanning electron microscopy with a Hitachi S-4800 high-resolution microscope.

Results

Variants of D-CONGA tested

We previously described the identification of the broad-spectrum, host-cell compatible antimicrobial peptide D-CONGA (**rrwarrlafafrr-amide**) by synthetic molecular evolution[5]. In this context, a "host-cell compatible" AMP is defined as one with antibacterial activity that is not inhibited by the presence of concentrated human erythrocytes[5, 7], which is meant to mimic *in vivo* conditions rich with host cells, protein, and tissue. Host cell compatibility is a rare property among known AMPs[5, 7] but is important to identify in AMPs designed to treat drug-resistant bacterial infections in wounds.

The iterative library from which D-CONGA was derived contained 28,800 members with some variation in the termini and in the core of the peptide, enabling tests of a number of specific hypotheses, described in detail previously[5]. In this work, we created a new set of rational variants to test new hypotheses for improving the activity or reducing the impediments to activity that were not included in the screen. The 13 amino acid sequence of D-CONGA (**rrwarrlafafrr-NH_2**), shown in **Fig. 2**, consists of critical double arginines on both termini, and a double arginine at positions 5 and 6. This creates a highly polar, but also amphipathic, N-terminal hexapeptide sequence of **rrwarr** which has five positive charges, including the N-terminus, plus the aromatic tryptophan. The C-terminal heptapeptide, **lafafrr**, has five consecutive nonpolar residues, including two large, aromatic Phe residues, making for a very hydrophobic, but also amphipathic segment. We previously showed that altering the hydrophobicity of this segment was deleterious. Decreasing hydrophobicity causes decreased antimicrobial activity, while increasing hydrophobicity causes increased toxicity[5].

In the new phase of evolution and optimization described here, we tested five classes of sequence variations of D-CONGA that had not been previously tested in a library or by rational variation. These are shown in **Fig. 2**. First, we made insertions at position 7 between the independent polar N-terminal and nonpolar C-terminal segments. Glycine and β-alanine were added to increase flexibility between segments, with β-alanine enabling maximum flexibility. We also inserted glutamine at position 7 to test the effect of extending the polar segment by one residue. Second, we tested the effect of deleting alanine residues at positions 4 and 10, because these two alanines had not been varied in any previous screen. These changes enabled the testing of shorter peptides. We also deleted the C-terminal arginine because DBS5 was found to be active without it[5]. Third, we added two amino acids with the opposite chirality within the sequence to assess the effect of interrupting secondary structure. By adding D-Arg residues to the N- and C-termini of an otherwise L-amino acid peptide, we are also testing the possibility of engineering protease resistance by terminal modification[23] without using D-amino acids for the whole peptide. The other such peptide had L-amino acids at positions 5 and 10 in the context of an otherwise D-amino acid sequence to test the importance of the secondary structure, which will be interrupted by this change. We also made a peptide in which we swapped the N- and C-terminal halves. Fourth, we made cyclized versions of L-CONGA by coupling the N-terminal amino group to either the C-terminus of an L-CONGA peptide acid, or to the sidechain of a C-terminal Asp residue on an L-CONGA peptide-

amide. Cyclization is an alternate way of reducing proteolysis on an L-amino acid peptide. Fifth, we tested peptides in which the Arg residues at positions 5 and 6 were replaced with Arg variants with longer or shorter versions of the guanidine-containing sidechains, homo-arginine and nor-arginine, respectively.

All variants were synthesized and purified as described previously[5, 7]. They were tested in broth dilution in the presence and absence of $1x10^9$ human RBCs per ml, 20% of the concentration in human blood, against *Escherichia coli*, *Klebsiella pneumoniae* and *Staphylococcus aureus*. See **Fig. 3A** for MIC values of the variants, compared to D-CONGA which is shown in the top row. *K. pneumoniae* and *S. aureus* were tested here because of their relatively lower sensitivity to D-CONGA. The toxicity of the variants was tested by measuring hemolysis and cytotoxicity against human WI-38 fibroblast cells. In **Fig. 3**B, we compare the antibacterial activities and toxicities of the variants to D-CONGA.

Identification of D-CONGA-Q7, a significantly improved variant

Most of the 13 variants had poorer average antibacterial activity than D-CONGA, **Fig. 3.** Seven variants lost useful activity against *S. aureus*, and a few of these also lost activity against *K. pneumoniae* and *E. coli*. Cyclization had the largest detrimental effect on activity, with both cyclic variants being almost inactive. Most deletion variants and those formed by addition of amino acids with different chirality also had poorer activity. The variants D-CONGA-ΔA4, -G7 and -HomoR had the same average MIC as D-CONGA**.** Only two variants had overall improved antibacterial activity, the insertion variant D-CONGA-Q7 and the flipped D-CONGA-FLIP.

Four variants had toxicity against fibroblasts that was similar to D-CONGA-Q7, while six were less toxic than D-CONGA. Toxicity values are plotted against average MIC values in **Fig. 3**B. The insertion variants, D-CONGA-G7, and -Q7, the deletion variant -ΔA4, the Arg variant -norR, and D-CONGA-FLIP were at least as good as D-CONGA in both categories, but only D-CONGA-Q7 was significantly improved in both categories. In the next sections, we carefully compare the important activities of D-CONGA and its best variant D-CONGA-Q7 to demonstrate that D-CONGA-Q7 displays a significant gain-of-function over D-CONGA.

Activity against clinical isolates of Gram-negative pathogens

Against laboratory strains of bacterial pathogens, D-CONGA-Q7 is measurably better than D-CONGA, **Fig. 3**. However, a much bigger gain of function was observed when we compared their activities against clinical isolates of drug-resistant bacteria, with a focus on *K. pneumoniae*, a

species of Gram-negative bacteria of rising concern that can show innate resistance to AMPs[24-26]. Two independent sets of isolates were tested, described above.

In **Fig. 4** we show the minimum inhibitory concentration (MIC) of eight conventional antibiotics and the two peptides, D-CONGA and D-CONGA-Q7, against the first set of isolates. The MIC values, shown in **Fig. 4A,** demonstrate the degree of drug resistance. All isolates are completely resistant to ceftazidime and ampicillin (MIC>150 μM), and 4 of the 14 isolates are resistant to all eight conventional antibiotics tested. D-CONGA, which has excellent activity (MIC ≤ 10 μM) against laboratory strains of all ESKAPE[27] pathogens, including K. pneumoniae, has poor MIC ≥ 20 μM against 5 of the 14 isolates (36%). Two isolates of *K. pneumoniae* are resistant to D-CONGA as well as to all conventional antibiotics tested. In sharp contrast, D-CONGA-Q7 has substantial activity against all isolates. MIC values for D-CONGA-Q7 are lower than for D-CONGA for all 14 isolates. No isolates have MIC ≥ 14 μM, for D-CONGA-Q7 and 13/14 have MIC ≤ 10 μM. In **Fig. 4B** we plot the fraction of isolates sterilized as functions of antibiotic concentration. The extraordinary activity of the new variant D-CONGA-Q7 is shown by the fact that half of these clinical isolates are sterilized by 2 μM D-CONGA-Q7 and 12/14 (86%) are sterilized by 5 μM. In comparison, the best conventional antibiotic, ciprofloxacin, is active against only 8 of the 14 isolates, or 57% at 100 μM.

To verify these results, we tested D-CONGA and D-CONGA-Q7 against a second, completely independent set of previously described clinical isolates of *K. pneumoniae*[14-15]. The results, in **Fig. 5A,** show the same behavior as above. For *K. pneumoniae* isolates, 7/19 (37%) are resistant to D-CONGA up to 25 μM, and only 2/19 (11%) have MIC < 5 μM. Validating our observations with the first set of isolates, the activity of D-CONGA-Q7 against these isolates is much better. For example, only 1/21 (5%) of strains are resistant to D-CONGA-Q7, and and 9/21 (57%) have MIC < 5 μM. See **Fig. 5**B.

Antibiofilm activity of D-CONGA-Q7

We reported previously[5] that D-CONGA has significant activity against biofilms formed by Gram-negative *P. aeruginosa* and Gram-positive *Streptococcus mutans.* Here, we directly compare the antibiofilm activity of D-CONGA and D-CONGA-Q7 using a mature pellicle biofilm of *P. aeruginosa*[17]. Pellicle biofilms are amenable to imaging by confocal laser fluorescence microscopy (CLFM) and to harvesting, which can be desirable for additional biofilm analysis, including counting of viable cells[16-17]. To determine the susceptibility of pellicle biofilms to D-CONGA and

D-CONGA-Q7, we cultured 2-days old biofilms as described in Methods. The coverslip-adhered biofilms were exposed to challenge solution for 24 h prior to staining with SYTOX red and imaging with CLFM, **Fig. 6**. The images obtained from biofilms treated with D-CONGA or D-CONGA-Q7, **Fig. 6A,** show viable cells (yellow) in the untreated control and a concentration-dependent decrease in viable cells, concomitant with an increase in dead cells and extracellular DNA (red), when biofilms are treated with each of the peptides. The % cell survival was quantitated as follows: (i) COMSTAT was used to compare biofilm biomass in CLFM images by estimating the biofilm biovolume, which is calculated as the overall volume/substratum area ($\mu m^3/\mu m^2$)[20-21]. Hence, % cell survival in each of the conditions is expressed as the ratio (untreated biomass)/(treated biomass). (ii) The biofilms were dispersed mechanically for subsequent enumeration of viable cells, such that % survival is expressed as the ratio ($CFU_{untreated\ biofilm}/CFU_{treated\ biofilm}$). The results obtained using COMSTAT and viable cell enumeration are shown in Figs. 5B and 5C, respectively. Both assays validate the previous reports of potent antibiofilm activity by D-CONGA. More importantly for this work, the data show that D-CONGA-Q7 is consistently more potent than D-CONGA, reducing viable biofilm bacteria by ≥90% at 8 μM peptide.

In **Fig. 7**, we show a direct comparison of the antibiofilm activity of D-CONGA and D-CONGA-Q7 to the clinically used lipopeptide antibiotic, colistin. Both synthetically evolved peptides are substabntially more active against P. aeruginosa biofilms than colistin. For example, while colistin shows no detectable activity at 2 μM, D-CONGA reduces biofilm CFU by 20% and D-CONGA-Q7 reduces biofilm CFU by 70%, at the same concentration.

***In vivo* antibacterial activity of D-CONGA-Q7 in a murine wound model**

D-CONGA-Q7 was tested in a murine wound model that we used previously to characterize D-CONGA[5]. In this model, a deep surgical punch wound, created on the dorsal surface of healthy adult CD1 mice is stabilized with a silicone ring to prevent healing by contraction, and then, covered with a Tegaderm dressing. The wound bed, with a volume of ~20 μL, is immediately infected with $1x10^5$ cfu of luciferase-*producing P. aeruginosa* or MRSA. Within hours the wound bed is purulent and has a high bacterial burden[5, 28], creating a challenging cell- and protein-rich environment to test AMP activity. Wounds are treated with 75 μg of D-CONGA-Q7 in 20 μL of water with 0.025% acetic acid every 8 hours for the first 5 days. The Tegaderm dressing are removed on day 3 post-infection and fixed in 2.5% glutaraldehyde for scanning electron

microscopy (SEM) analysis of wound biofilms. The use of luminescent bacteria enables daily monitoring of bacterial burden in the wounds of each individual animal, as shown by the images in **Fig. 8A** and **8B**. Integrating the luminescence across the wound bed each day allows wound bacterial burdens to be monitored over time. Thus, in this model system, the relevant measure of peptide effect is the reduction in bacterial burden across the peak of infection on Days 1-3. Compared to the activity of D-CONGA[5] the activity of D-CONGA-Q7 is equivalent, with ≥4 logs of maximum reduction of MRSA burden and ~2 logs of reduction of *P. aeruginosa* burden, **Fig. 8C&8**D. Other wound criterion scores, shown in Supplemental **Fig. S1**, demonstrate that wound appearance and healing are similar in controls and peptide treated samples, showing that the peptide is not causing tissue damage, despite its high local concentration.

Preliminary data had shown that once per day treatments in simple aqueous vehicle was ineffective against wound infections in this model, see **Fig. S2.** Therefore, we also tested the effectiveness of D-CONGA-Q7 formulated in aqueous polymer suspensions of carboxymethyl cellulose and Xanthan gum, which are both long anionic carbohydrate polymers that create highly viscous solutions. These viscous solutions were applied to the wound once per day. A once per day treatment regimen using this simple formulation was effective at reducing bacterial burdens, **Fig. S3**, demonstrating that clinically useful formulations of these peptides may be straightforward to develop.

D-CONGA-Q7 activity against wound biofilms in vivo.

The Tegaderm dressing used in the murine wound model is an excellent substrate for bacterial adhesion and biofilm formation[5, 28]. In the wound experiment, the dressing is removed on Day 3 post-infection and fixed, followed by electron microscopy analysis. We image 3-4 randomly selected areas of each Tegaderm sample at two magnifications each. Each image is scored for the presence/absence of bacterial cells, either rod-shaped *P. aeruginosa*, ~1 μm diameter, or spherical MRSA cocci, ~0.9 μm in diameter. Images are also scored for biofilm-like structures defined by having multiple bacteria embedded in an obvious three-dimensional matrix. These distinctions are not subtle, as shown by representative images of the fixed Tegaderm dressings in **Fig. 9A** and **9B**. In vehicle control samples, we observed that *P. aeruginosa* frequently forms an open, three-dimensional matrix in which cells are entangled in many μm-long fibers. We observed that MRSA, forms a matrix in which cells are close-packed in strands that comprise a large-scale mesh. We performed a statistical analysis of observed bacteria and biofilms using the binomial equation.

Results are shown in **Fig. 9C.** Every SEM image (68/68) from vehicle control samples of the two bacteria contained obvious visible bacteria, and most of these images contained ≥ 50 individual cells. In samples from Q7-treated animals, 57 of 68 (84%) of images had no bacteria. Less than 50 bacteria were observed in each of the remaining 11 of 68 (16%) of total images. Apparent biofilms were observed in 43/68 (63%) of vehicle treated samples, while no biofilm was observed in the 68 images from D-CONGA-Q7-treated animals. P-values for all comparisons of treated vs vehicle were less than 0.001.

Discussion

The overarching clinical challenge of our continued evolution of novel AMPs is to protect and treat wounds, especially chronic wounds infected by drug-resistant bacteria. We are approaching this result by evolving peptides as new antibacterial chemotypes that are effective against multispecies infections and wound biofilms formed by drug-resistant bacteria in the very complex protein and cell-rich environment of an infected wound[5]. For example, current standards of care for diabetic ulcers and other chronic wounds are not effective at preventing the high rate of serious complications, especially chronic infection[29-32]. These common treatment failures are costly and negatively impact quality of life. Ultimately, complications from chronic wounds lead to a cumulative probability of limb amputation of about 16% of US diabetics[33-34]. Effective treatment for infected wounds would reduce the burden on both patients and healthcare facilities.

Yet, clinical use of AMPs requires that impediments be circumvented and antibacterial activity optimized. Despite decades of research into antimicrobial peptides, and many thousands of distinct sequences described[4], there is a striking absence of useful or quantitative sequence-structure-activity rules (QSAR) for any of the activities or impediments, making simultaneous parallel optimization a hopeless undertaking. Even machine learning approaches have not yet demonstrated the ability to predict clinically useful AMPs. One reason for the absence of useful QSAR is that membranes are two-dimensional fluids and peptides act on them as a dynamic ensemble of heterogeneous structures[8]. AMPs do not self-assemble into specific unique pore structures, and do not act by forming explicit pores in membranes[35-36]. Instead, AMPs accumulate massively on bacterial membranes and destabilize the membrane lipid packing by a physical-chemical process that we have called "interfacial activity"[8]. The dependence of AMP activity on non-specific, dynamic and heterogeneous structures inhibits rational optimization. The properties

of these ensembles are sensitive to many experimental details, leading us to suggest that they are best described by the concept of a "mechanistic landscape"[37] rather than by a defined set of structure-function rules.

To discover new antimicrobial peptides in the absence of useful QSAR, one must resort to trial and error. In this spirit, we have been optimizing the family of AMPs discussed here using multiple iterative generations of library screening and rational hypothesis testing. Here, we describe the properties of the most recent generation of rational variants of the evolved, host-compatible AMP D-CONGA.

Most variants of D-CONGA have equal or less activity

Interestingly, the three bacteria tested had different susceptibilities to changes in the sequence of D-CONGA. *E. coli*, against which D-CONGA was highly active, was the least sensitive to changes. The majority of variants have MIC that are within a factor of two of the MIC for D-CONGA. *K. pneumoniae* had a much wider range of changes, probably because the parent MIC values are not as low as for *E. coli*, enabling some improvement for some variants. About a third of the variants were significantly better than D-CONGA against *K. pneumoniae*, and most of the remaining variants were similar. *S. aureus* showed the most sensitivity to sequence changes, a phenomenon that we have reported previously[5]. Half of the variants lost all activity against this organism, and only two variants were better than D-CONGA.

Among the variations of D-CONGA tested, the most dramatic loss of antimicrobial activity was observed for the cyclized peptides. These variants have much lower activity than D-CONGA against two or three of the organisms tested, including against E. coli. These results may reveal the importance of linear amphipathicity on activity for this peptide lineage. Having double arginines on both N- and C-termini was one of the most strongly selected features of previous screens[5, 11]. The cyclic variants place these arginines in a contiguous location in the ring, breaking the amphipathicity.

The two alanine deletion variants show an example of the unexpected information that can be obtained from rational changes like those we explored here. These two variants were made with deletions of alanine residues that had not been varied since they were selected in the first generation screen (**Fig. 1**). Deletion of the alanine at position 4, in the N-terminal polar RRW**A**RR sequence, had essentially no effect on antimicrobial activity or on cytotoxicity. On the other hand, deletion of the alanine at position 10, which is in the C-terminal non-polar segment LAF**A**FRR caused a

significant reduction in antimicrobial activity, especially against *S. aureus*. This agrees with our hypothesis that the net length and hydrophobicity of the C-terminal segment are critical for activity. Other observed changes are inexplicable. For example, several seemingly unrelated variants lost all activity against S. aureus, while maintaining activity against the two Gram-negative pathogens. These include the β-alanine insertion at position 7, as well as ΔR13 and the peptide with D-amino acids at positions 5 and 10 in an otherwise L-amino acid sequence (see above).

D-CONGA-Q7 is a gain-of-function variant

Two variants of D-CONGA had substantially better activity against the three organisms in **Fig. 3**; D-CONGA-Q7, with a polar glutamine inserted between the N-terminal polar and C-terminal hydrophobic segments, and D-CONGA-FLIP in which the two segments were swapped. Of these two, only D-CONGA-Q7 also had lower cytotoxicity against fibroblast cells. Therefore, we selected D-CONGA-Q7 as the lead peptide for additional studies against clinical isolates, against biofilms, and in our animal model of infected wounds. As described above, we found that D-CONGA-Q7 is equal or superior to D-CONGA in every measurement.

Resistance avoidance

When selecting the two sets of clinical isolates to study we focused on *K. pneumoniae*, a Gram-negative pathogen for which drug resistance is a serious and growing public health threat[24]. Among the clinical isolates tested, some were from pulmonary reservoirs in cystic fibrosis patients [38-40]. These strains, subjected to years of antibiotic treatment, frequently activate multiple parallel mechanisms of pan drug resistance[40].

We had previously passaged *P. aeruginosa* against D-CONGA over many generations and found no change in susceptibility[5], indicating that resistance is slow to arise against this peptide. In parallel experiments, resistance of *P. aeruginosa* to multiple conventional antibiotics grew rapidly over just a few passages[5]. Therefore, while the Gram-negative *K. pneumoniae*, like *P. aeruginosa*, can become resistant to some AMPs by mechanisms that affect the net charge and architecture of the outer membrane lipid A and LPS[13, 41-43] we did not expect resistance to D-CONGA. Furthermore, other authors have reported that resistance to conventional antibiotics is strongly correlated with "widespread collateral sensitivity" to AMPs[44], so we expected the clinical isolates to be sensitive to D-CONGA.

Yet, against the *K. pneumoniae* isolates, we were surprised to observe that more than half were resistant to D-CONGA despite its good activity against other strains[5]. We were equally surprised when, against the same *K. pneumoniae* isolates, D-CONGA-Q7 was much more effective, with 28 of 29 *K. pneumoniae* isolates susceptible to D-CONGA-Q7. This superior activity was observed despite not specifically selecting for resistance avoidance in this round of variations and testing. Further studies will be required to understand the mechanistic basis for the resistance avoidance of D-CONGA-Q7 against *K. pneumoniae* isolates. These insights will be very important to the advance of resistance avoiding AMPs into the clinic.

Acknowledgments. AS and MR were supported by NIH grants AI125529 and AI169344**.** WW, LM, and JK were supported by NIH grant AI154284. JK was supported by the Louisiana Board of Regents Endowed Chairs for Eminent Scholars program, Cystic Fibrosis Foundation grant KOLLS21I0, as well as by PHS grant R35HL139930 and NIAID/NIH award R01AI114697.

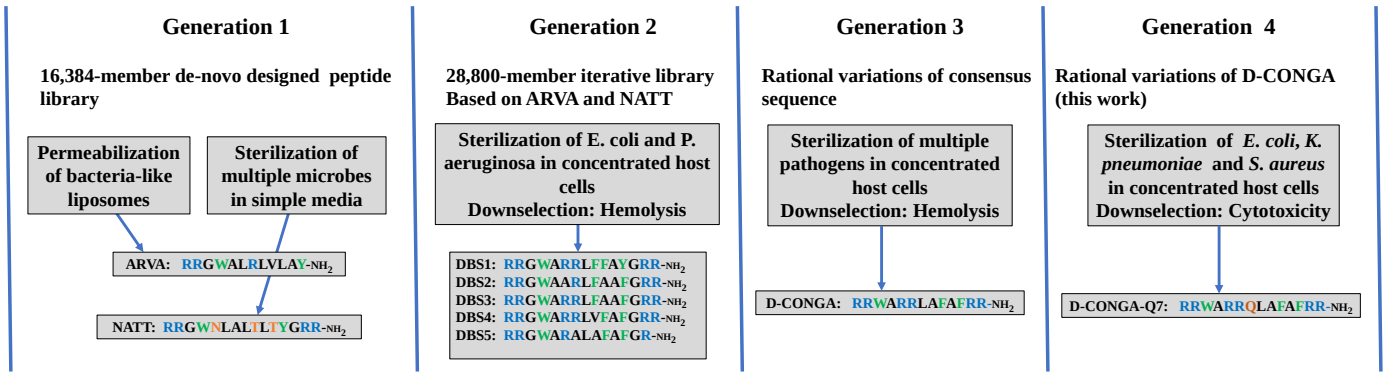

Figure 1. History of the evolution of the AMPs discussed here. The first generation de novo library was screened for liposome permeabilization[9-10] and antimicrobial activity[11]. The two families of AMPs derived from generation 1 were used to design a library, which was screened for host-compatible AMP activity[5]. A round of rational variants was tested to identify D-CONGA, a host compatible AMP with highly promising activities *in vitro* and *in vivo*[5]. Generation 4 is the work described here.

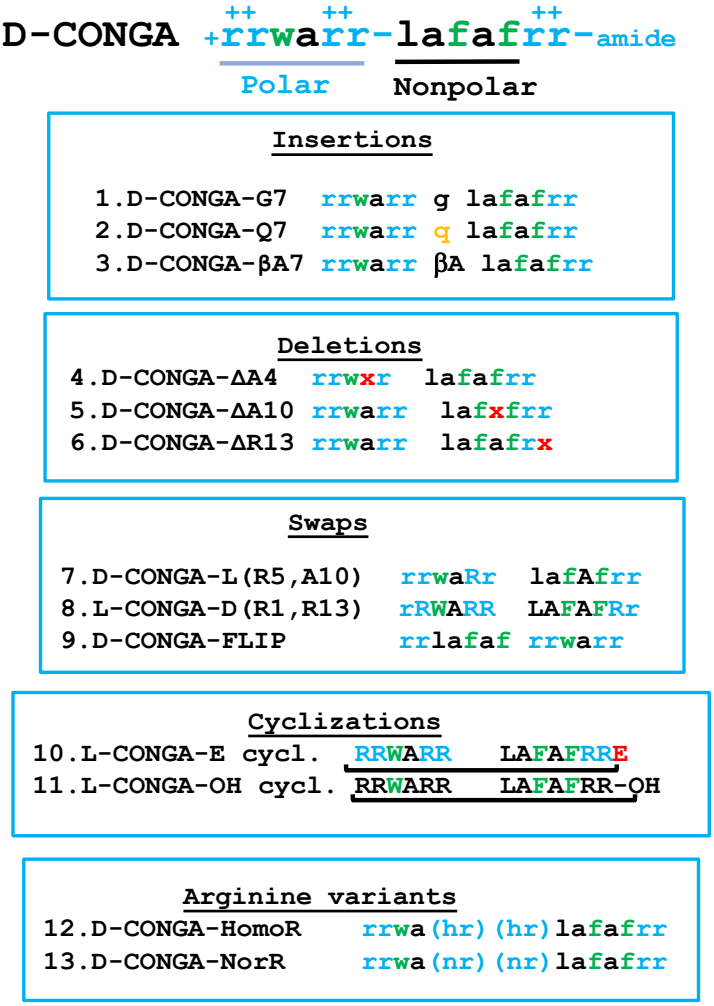

Figure 2. Design and synthesis of D-CONGA variants. 13 rational variants of D-CONGA were synthesized and tested here. The variants can be divided in to five broad groups based on the modification in the sequence of D-CONGA. Insertions were made by adding an amino acid to D-CONGA sequence after the R residue at position 6. This position is denoted by a hyphen in the D-CONGA sequence above. Deletions were made by removing an amino acid from D-CONGA that had not been previously varied. Swaps contain 3 variants with position and enantiomer exchanges within CONGA. Cyclized peptides are two variants made by the cyclization of D-CONGA. Arginine variants replace the RR motif at positions 5 and 6 with Arginine analogs with shorter and longer sidechains. Norarginine, has one additional methylene unit and homoargoinine has one fewer methylene unit.

A

Peptides	*E. coli*		*K. Pneumoniae*		*S. Aureus*		Mean MIC µM	Hemolysis at 100 µM	EC50, µM
	MIC in Broth Dilution, µM							RBC	WI-38
+/- 10^9 RBC/ml	-	+	-	+	-	+			
D-CONGA	1.0	0.8	4.4	3.8	5.7	6.3	3.7	0.06	110
D-CONGA-G7	1.3	1.4	1.7	4.4	6.4	6.9	3.7	0.07	235
D-CONGA-Q7	1.0	1.7	1.1	1.5	4.2	3.6	2.2	0.07	418
D-CONGA-βA7	1.0	1.3	1.4	1.5	>30	>30	16	0.02	>1000
D-CONGA-ΔA4	1.6	2.8	4.5	6.2	3.2	2.3	3.4	0.02	143
D-CONGA-ΔA10	0.7	1.3	1.6	>30	24	19	15	0.02	257
D-CONGA-ΔR13	0.9	0.6	2.1	2.1	27	>30	13	0.03	300
D-CONGA-FLIP	1.0	1.5	1.2	1.4	1.7	3.7	1.8	0.05	143
D-CONGA-L-R5,A10	1.4	1.4	2.3	2.2	>30	>30	16	0.04	>1000
L-CONGA- (R1,R13)	20	26	5.1	9.3	>30	>30	25	0.01	134
L-CONGA-E cycl.	23	>30	20	>30	>30	ND	36	0.03	ND
L-CONGA-OH cycl.	5.9	13	2.9	6.0	20	ND	9.6	0.07	ND
D-CONGA-HomoR	1.3	2.2	8.0	5.4	1.7	2.5	3.5	0.06	143
D-CONGA- NorR	1.9	2.4	13	12	7.6	17	9.0	0.03	66

B

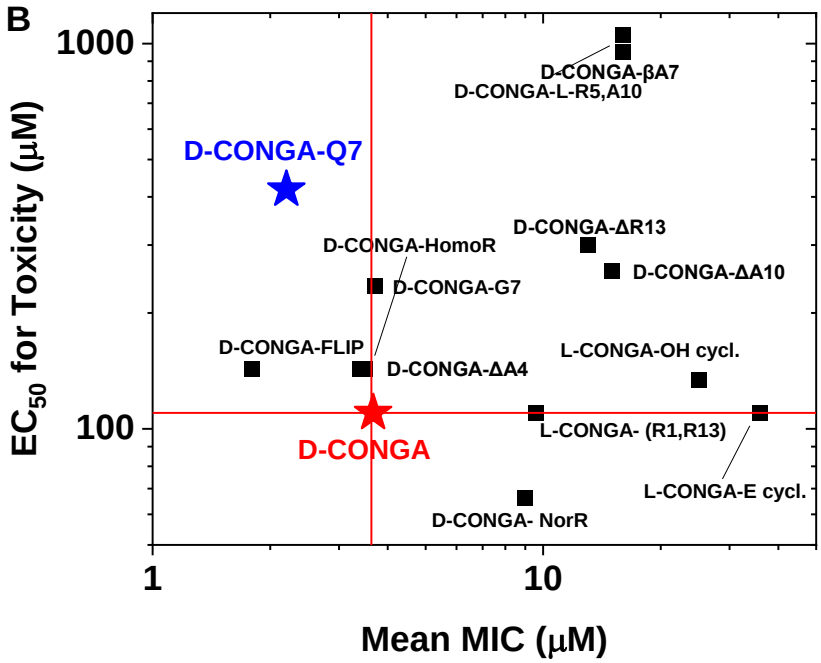

Figure 3. Characterization of D-CONGA variants. A. MIC values are reported in µM peptide against gram-negative *E. coli* (EC), *K. pneumoniae* (KP), and the gram-positive pathogen *S. aureus* (SA). The two columns under each organism are for assays performed in the absence (-) and presence (+) of $1x10^9$ human RBC/ml. MIC color codes are as follows: Yellow: Values are similar to that of D-CONGA. Green: Values are better than D-

CONGA.Red: Values are worse than D-CONGA (higher MIC and hemolysis, lower EC_{50}). “>30” means that sterilization was not observed at 30 μM, the highest concentration tested. The column marked “hemolysis” is the fractional hemolysis of $1x10^8$ human RBCs/ml at 100 μM peptide determined from measurements of serially diluted peptide, starting from 100 μM. The column marked “EC_{50}” contains the concentration of peptide that kills 50% of WI-38 human fibroblast cells assayed by entry of SYTOX Green, a DNA binding dye.

Compound	Abbr.	Class/Target
D-CONGA	--	AMP
D-CONGA-Q7	--	AMP
Gentamycin	GEN	Aminoglycoside
Ceftazidime	CAZ	Cephalosporin
Ampicillin	AMP	Beta-lactam
Ciprofloxacin	CIPRO	Fluoroquinolone
Tobramycin	TOB	Aminoglycoside
Trimethoprim	TMP	DHFR Inhibitor
Ceftriaxone	CRO	Cephalosporin
Meropenem	MEM	Carbopenem

Table 1. Conventional antibiotics and clinical isolates. The antimicrobial activity of D-CONGA and D-CONGA-Q7 was compared to eight conventional antibiotics from four different classes against drug resistant clinical isolates of *K. pneumoniae*, *P. aeruginosa*, *Acinetobacter baumanii*, and *S. aureus*.

A

	AMPs		Antibiotics							
	D-CONGA	D-CONGA-Q7	GEN	CAZ	AMP	CIPRO	TOB	TMP	CRO	MEM
ID	MIC, µM									
K. pneumoniae and P. aeruginosa isolates										
KP 6	4.2	3.2	>150	>150	>150	9.4	>150	13.3	>150	0.2
KP 46	4.4	2.2	1.6	>150	>150	0.2	3.5	1.3	1.9	0.4
KP 398	32	3.8	1.9	133	>150	0.2	6.9	18	0.2	0.2
KP 2146NDM-1	15	1.8	>150	>150	>150	>150	>150	>150	>150	>150
KP ST396	2.0	1.9	2.0	>150	>150	0.2	4.6	124	1.9	0.3
KP ST258 C2	64	8.9	>150	>150	>150	>150	>150	>150	>150	>150
KP ST258 C3	92	14	>150	>150	>150	>150	>150	>150	>150	>150
KP ST258 I2	3.2	1.4	8.3	>150	>150	>150	>150	>150	>150	>150
KP (CRE)	23	2.0	5.2	>150	>150	>150	>150	>150	45	108
PA (mucoid)	4.4	4.2	5.5	116	>150	4.2	4.2	75	137	13.3
PA (non-mucoid)	1.3	1.1	8.3	>150	>150	5.6	5.9	75	89	4.0
Other Isolates										
KP ATCC 33495	5.0	2.4	1.9	>150	>150	0.2	7.5	124	0.3	0.2
MRSA USA400	2.6	1.5	>150	>150	>150	0.8	>150	3.2	>150	>150
AB (PDR)Tulane	2.4	1.1	>150	>150	>150	>150	>150	>150	>150	>150

B

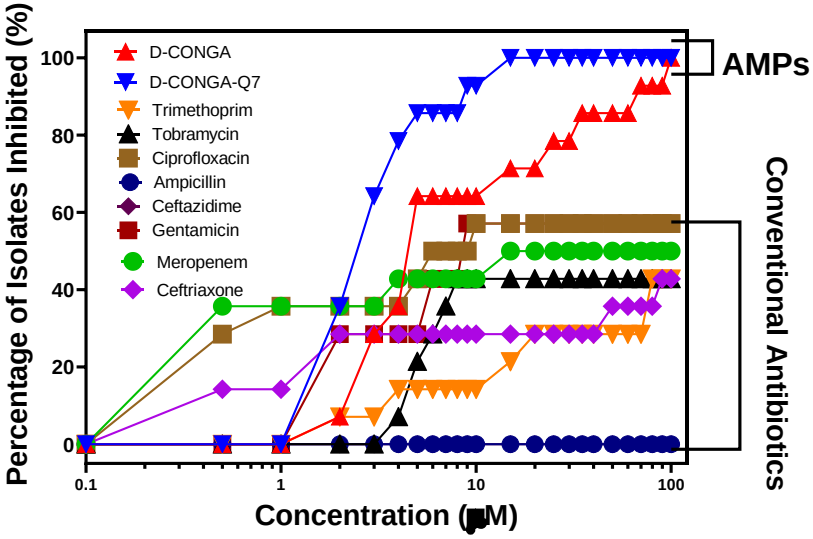

Figure 4. Activity of D-CONGA, D-CONGA-Q7, and conventional antibiotics against clinical isolates. A. MIC values in broth dilution are reported in µM concentrations against 14 clinical isolates of resistant bacterial strains. Color codes are as follows: Green: MIC ≤ 5 µM. Yellow: 5≤ MIC ≤ 20. Red: MIC ≥ 20 µM. “>150” means that sterilization was not observed at 150 µM, the highest concentration of antibiotic tested. **B.** Fraction of the 14 isolates sterilized versus antibiotic concentration.

A

ID	D-CONGA	D-CONGA-Q7	ID	D-CONGA	D-CONGA-Q7
K. Pneumoniae Isolate MIC (µM)					
1000527	>25	6.8	KP NIH 1	>25	6.8
1002565	>25	5.1	KP NIH 10	>25	>25
1100770	7.3	5.1	KP NIH 24	>25	6.8
1100975	14	3.4	KP NIH 27	>25	3.4
ATCC 43816	5.4	6.8	KP NIH 29	14	2.5
ATCC 700721	5.4	6.8	KP NIH 30	7.3	3.4
K6	2.7	3.4	KP NIH 31	7.3	3.4
K 6.1	14	3.4	KP NIH 32	>25	6.8
K 6.2	14	5.1	KP NIH 33	3.6	1.3
KP 80	14	3.4			

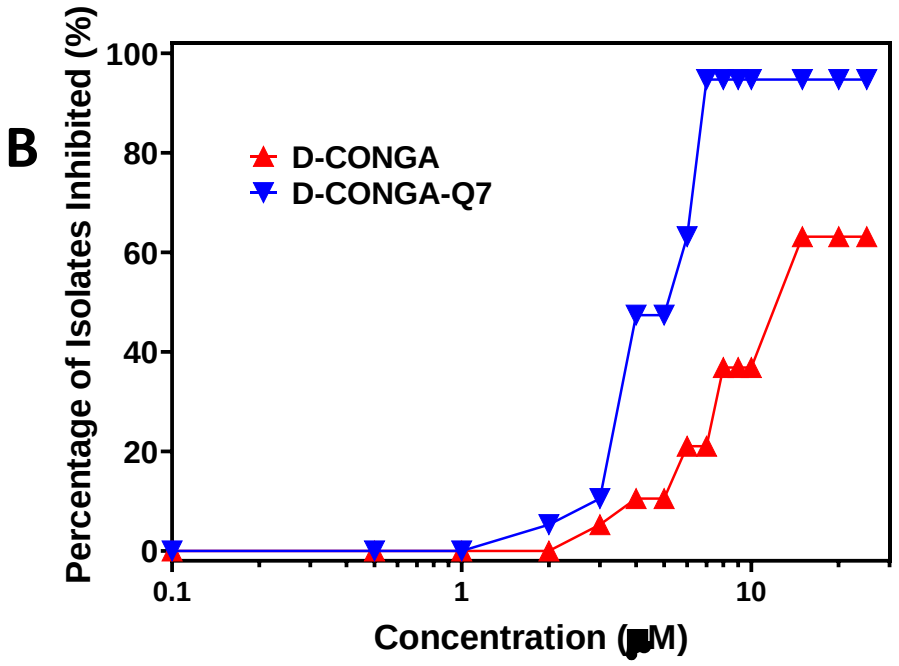

Figure 5. Activity of D-CONGA and D-CONGA-Q7 against an independent set of clinical isolates. A. Activity of D-CONGA and D-CONGA-Q7 against an independent set of clinical isolates of *K. pneumoniae* described elsewhere[14-15]. MIC values are shown in A. Yellow cells indicate MIC ≥ 8 µM, red cells indicate MIC ≥ 10 µM and green cells indicate MIC ≥ 5 µM. **B.** Fraction of the isolates sterilized versus antibiotic concentration.

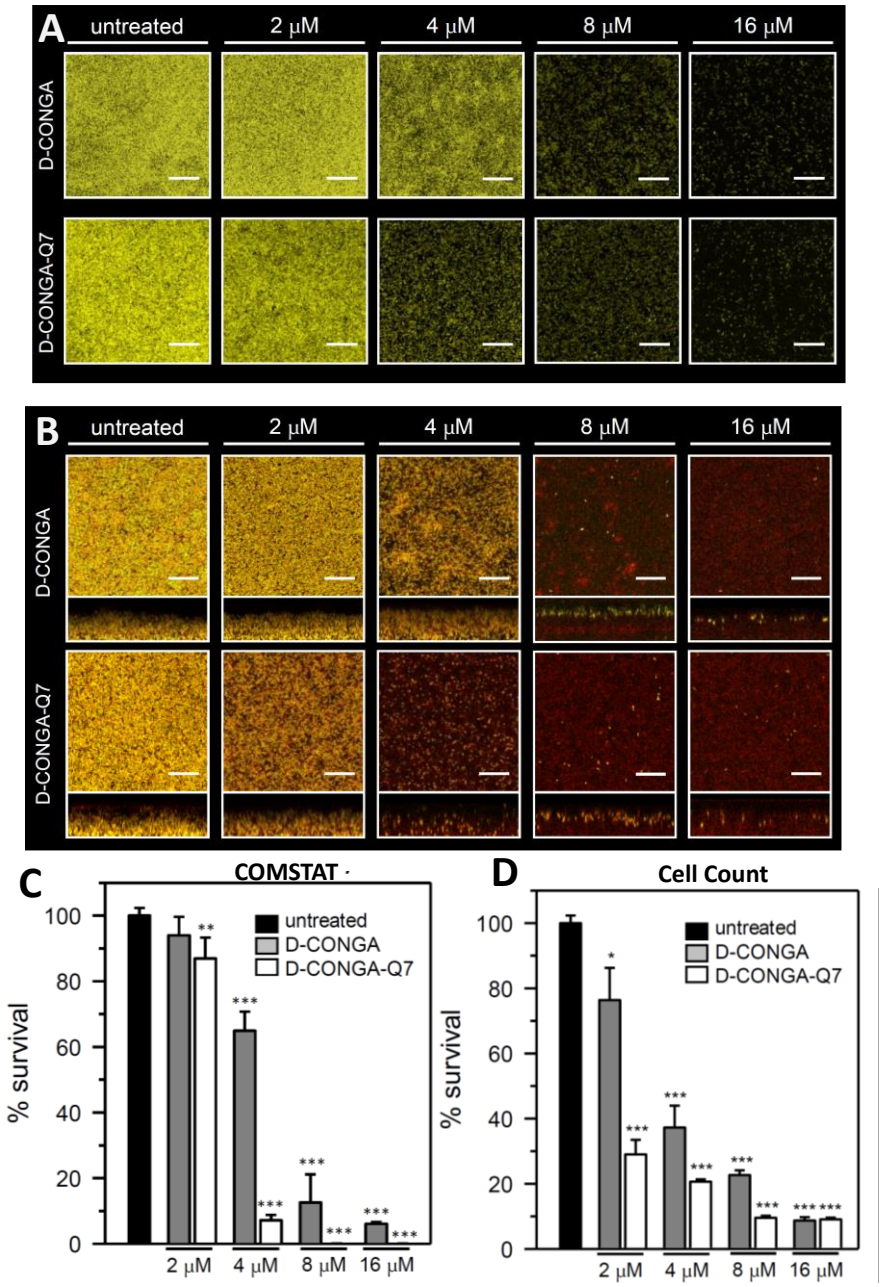

Figure 6. Antibiofilm activity of D-CONGA and D-CONGA-Q7. Pellicle biofilms of *P. aeruginosa* PAO1 expressing the enhanced yellow fluorescent protein (EYFP) were cultured for 48 h in PI media supplemented with 20 μM Fe and then treated for 24 h with different concentrations of peptide. For CLSM imaging, the biofilms were counterstained with Sytox Red and imaged. **A.** Images show the maximum projection of viable cells (yellow) after treatment. **B.** Images depict top-down (squares) and side views (rectangles) of viable cells (yellow), dead cells (red) and extracellular DNA (red). The scale of the bars represents 20 μm. **C.** The % cell survival

calculated from the CLSM images with the aid of COMSTAT software. **D.** The % cell survival calculated from CFUs after dispersing the biofilms and enumerating viable cells. $p < 0.1$ denoted by *, $p < 0.01$ by ** and $p < 0.001$ by *** relative to untreated.

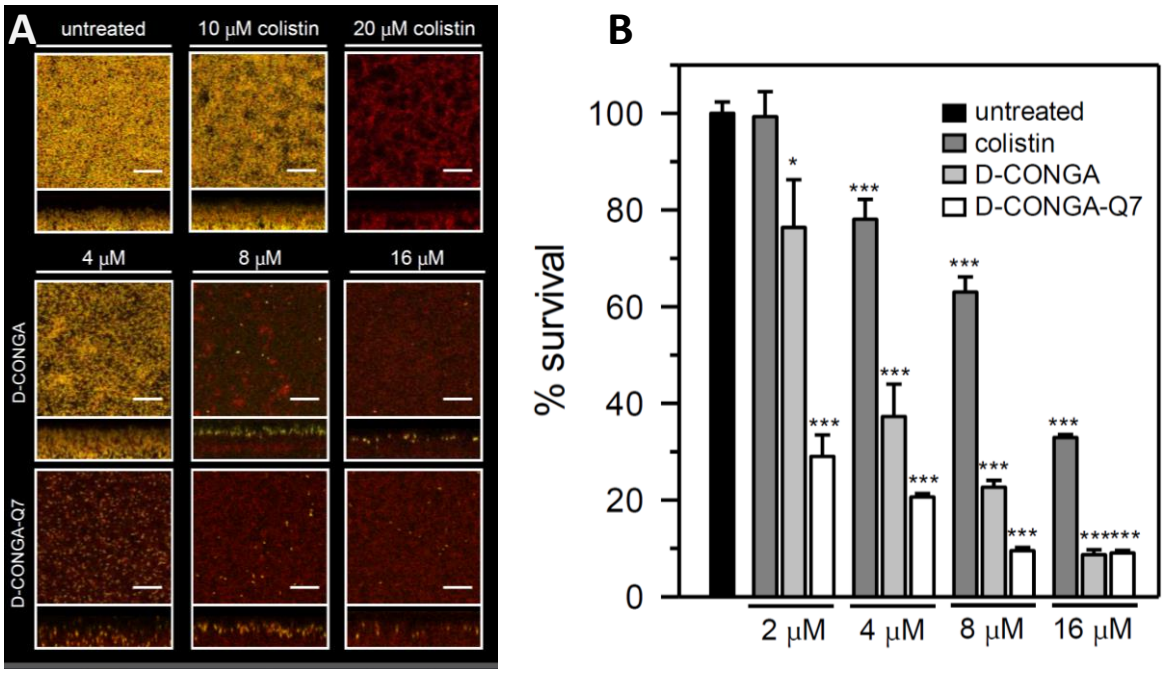

Figure 7. Comparison of the antibiofilm activity of D-CONGA and D-CONGA-Q7 with colistin. Pellicles of *P. aeruginosa* PAO1 expressing the EYFP were grown for 48 h in PI media supplemented with 20 μM Fe and challenged with peptides or colistin for 24 h. **A.** The biofilms were counterstained with Sytox Red and imaged by CLSM. Images depict top-down (squares) and side views (rectangles) of viable (yellow) and dead cells and extracellular DNA (red). The scale of the bars represents 20 μm. **B**. Comparison of cell survival in pellicle biofilms after treatment with peptides or colistin by dispersing and counting viable cells. The % survival is expressed as the ratio CFU/mL $_{(untreated)}$ / CFU/mL $_{(treated\ with\ peptides)}$. $p < 0.1$ denoted by *, $p < 0.01$ by ** and $p < 0.001$ by *** relative to untreated.

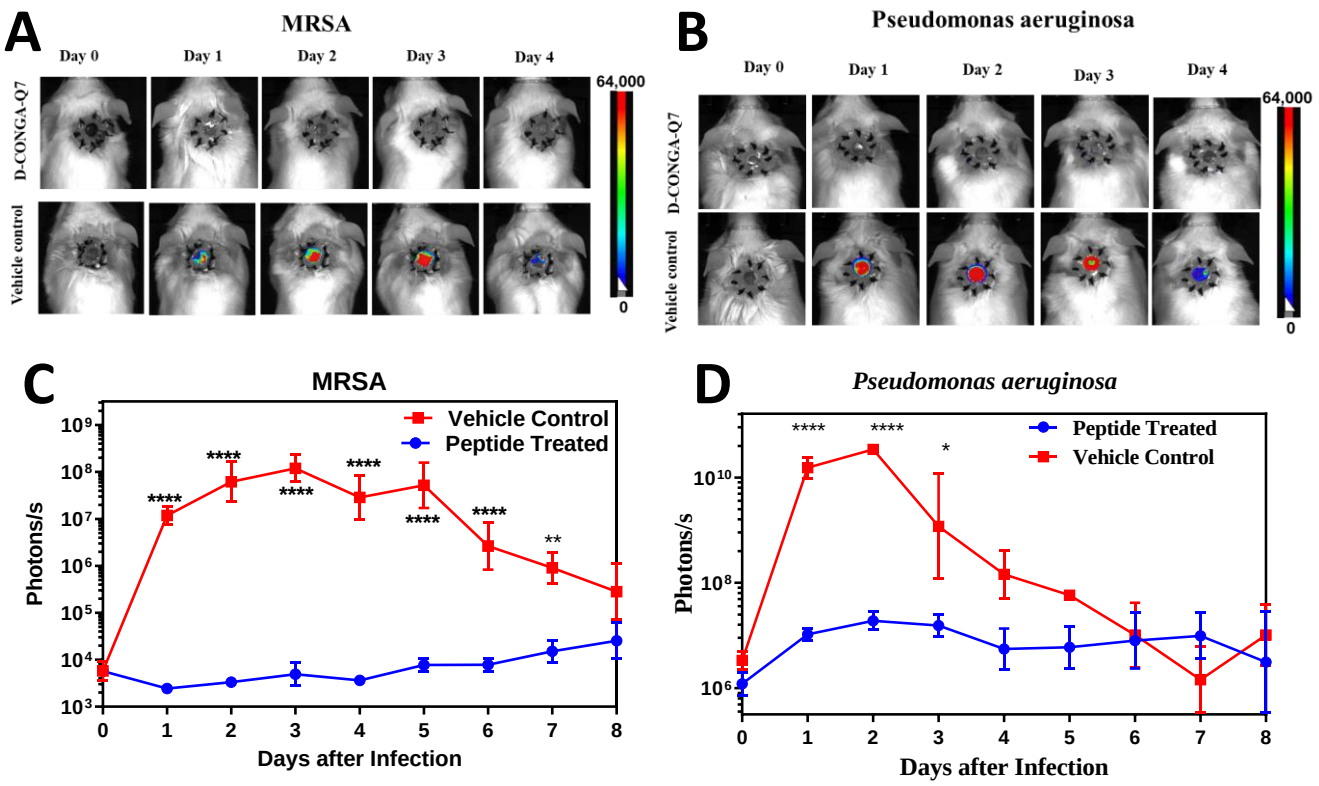

Figure 8. Animal model of deep surgery wound infection. Circular, dorsal puncture wounds were surgically created in healthy, adult CD1 mice, stabilized with a sutured silicon ring, and covered with Tegaderm dressing to better mimic infection and wound healing in humans. Wounds were infected with luminescent *P. aeruginosa* or luminescent MRSA and were treated with D-CONGA-Q7 peptide or vehicle control every 8 h until Day 4. An IVIS whole animal imager was used to measure luminescence in all animals once per day after infection. **A, B.** Example daily images of mice infected with luminescent *P. aeruginosa* or MRSA are shown, treated with PBS control or D-CONGA-Q7 **C, D.** Total integrated radiance from the wound bed was measured daily. Statistical significance between peptide and control denoted by asterisks.

Pseudomonas aeruginosa

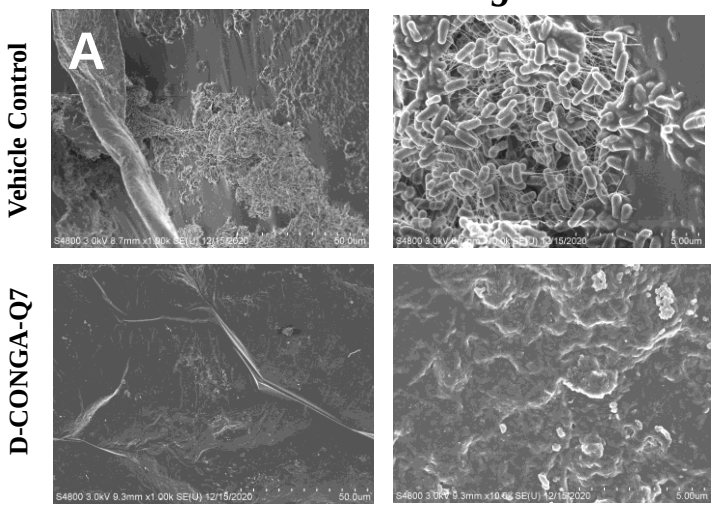

MRSA

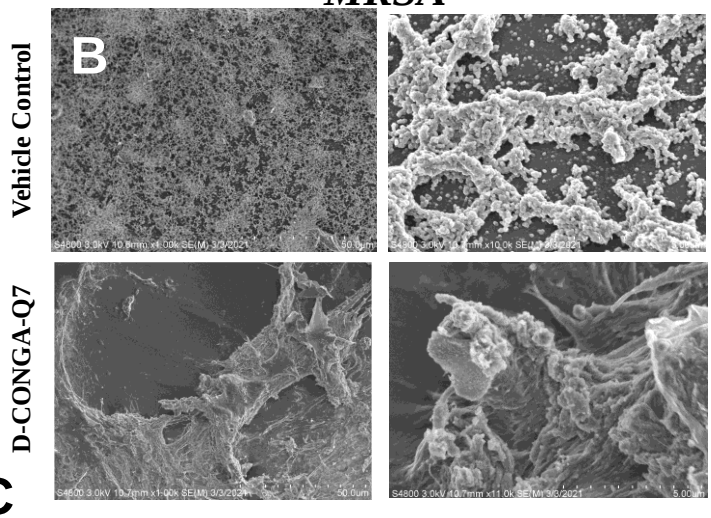

C

Treatment	Pathogen Species	
	P. aeruginosa	
	Bacteria present	Biofilm present
Vehicle	33/33	10/33
D-CONGA-Q7	8/33	0/33
p-value	>0.0001	0.0009
	MRSA	
	Bacteria Present	Biofilm present
Vehicle	35/35	33/35
D-CONGA-Q7	3/35	0/35
p-value	>0.0001	>0.0001

Figure 9. Wound biofilm reduction. A,B. Representative scanning electron microscopy images of glutaraldehyde-fixed Tegaderm dressing from *P.aeruginosa* infected mouse wound. The dressings removed from experimental animals on Day 3 are presented here in 1K and 10K magnifications. Scale bars are 5 μm in all images. The top two images show vehicle controls with abundant biofilms and rod-like *P.aeruginosa* in all samples. The bottom two images point on the tegaderm of wound treated 3 times a day with D-CONGA-Q7. They have few individual bacteria. No biofilm is observed, and only the tegaderm adhesive is visible. **C.** Counts of bacteria and biofilms observed in all random images of the Tegaderm dressing. P-values are determined from 2x2 contingency tables using Fisher's exact test.

SUPPLEMENTARY DATA

Figure S1 – Wound score

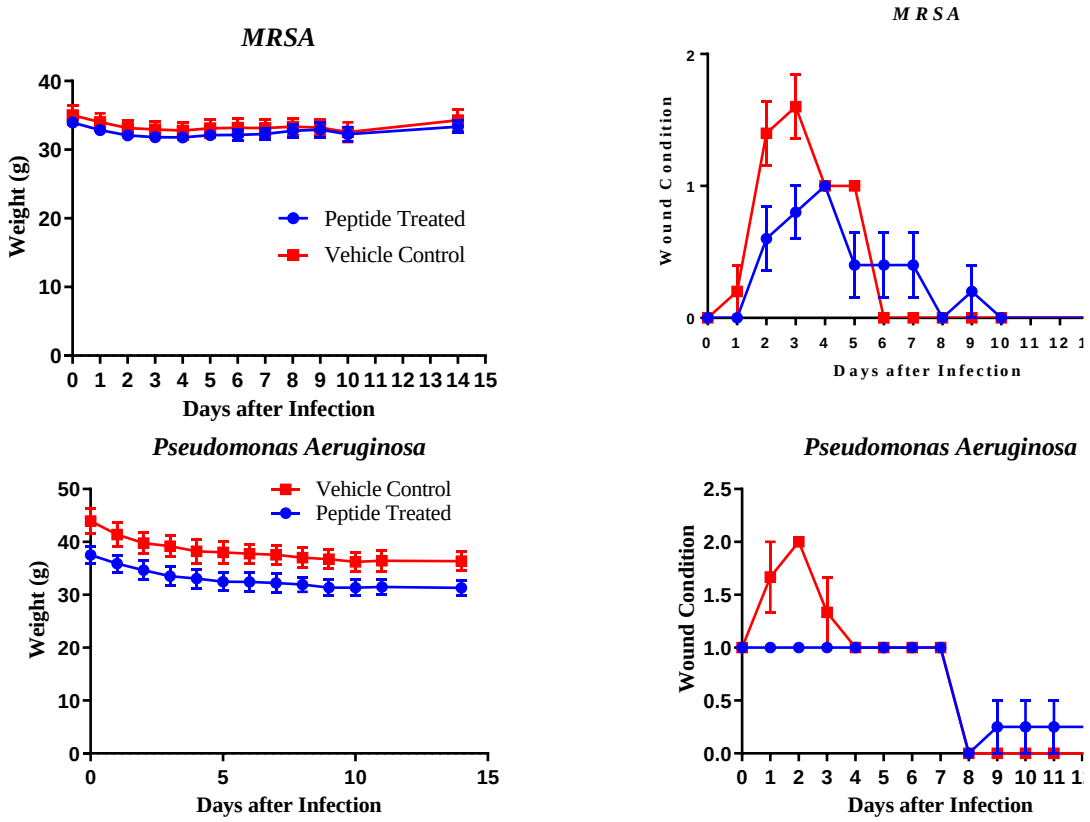

Figure S1. Post-surgery mouse monitoring data. A and C) The weights and **B and D)** wound condition of each mice was monitored every day for the 14 days of the experiment. Mice did not demonstrate any weight loss based on different bacterial infections or solvent treatments. In addition, there was no significant difference in the wound condition of mice treated with peptide versus those treated with vehicle control in *P.aeruginosa* and MRSA infected mice.

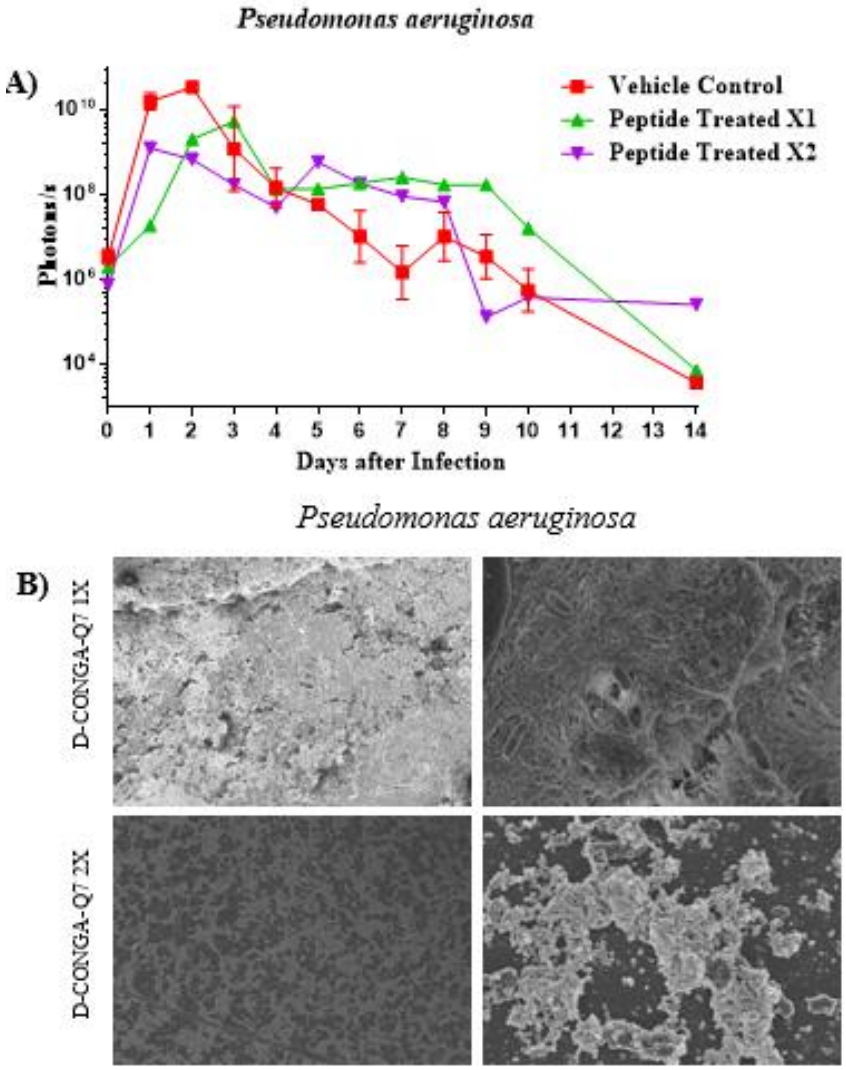

Figure S2. Activity of D-CONGA-Q7 in wound model using 1x and 2x per day administration. Bacterial burdens are not reduced significantly by once or twice per day administration, nor is Tegaderm biofilm formation inhibited. Results for three times per day administration, in which bacterial burden is greatly reduced and biofilm formation prevented, is described above in Fig. 8.

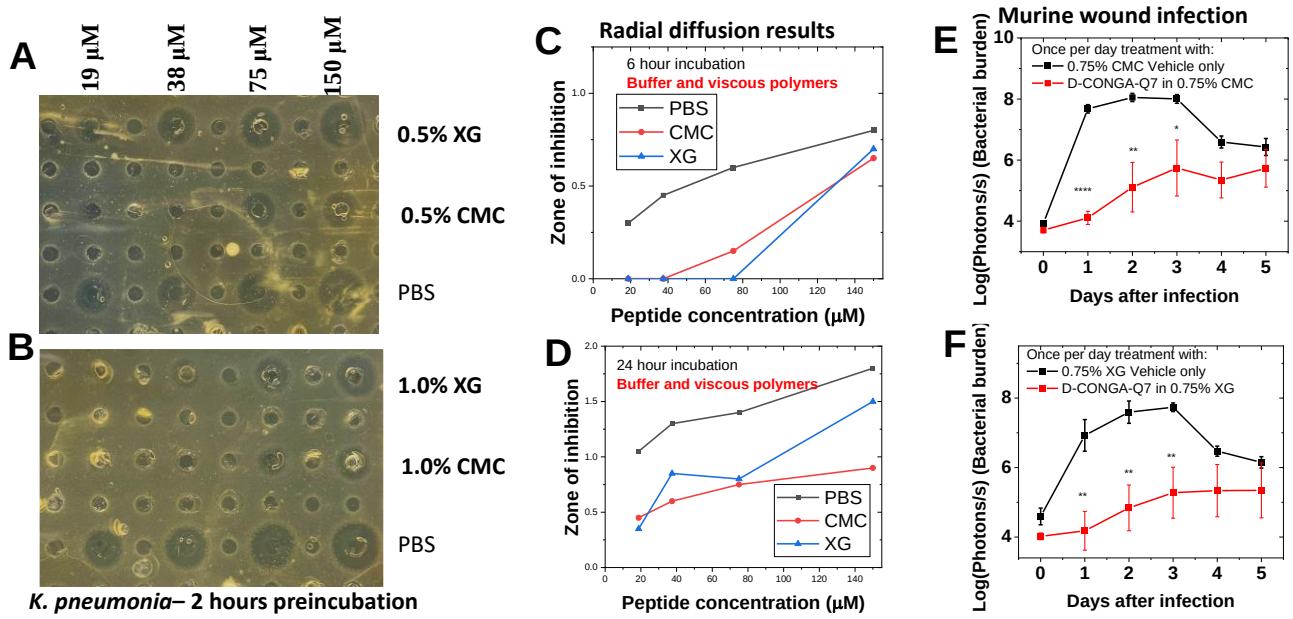

Figure S3. Activity of D-CONGA-Q7 once per day formulated with viscous polymers. **A-D.** In vitro characterization of formulated D-CONGA-Q7 using S. aureus in radial diffusion assays. Using 1% w/w suspensions of carboxymethylcellulose or Xanthan gum created formulations that effectively solubilized the peptide and slowed the release of peptide into agar plates for at least 24 h, compared to the vehicle, PBS. **E,F:** Wound model data for once per day administration of polymer stabilized formulations of D-CONGA-Q7 compared to vehicle PBS. Statistically significant reductions in wound bacterial burden was achieved with this once-per-day treatment.

1. Costa, F.; Teixeira, C.; Gomes, P.; Martins, M. C. L., Clinical Application of AMPs. *Adv Exp Med Biol* **2019,** *1117*, 281-298.

2. *Antimicrobial Peptides. Basics for Clinical Application*. Springer: Singapore, 2019; Vol. 1117.

3. Naafs, M., The Antimicrobial Peptides: Ready for Clinical Trials? *Biomedical J Sci & Tech Res* **2018,** *7*, 001536.

4. Wang, G.; Li, X.; Wang, Z., APD3: the antimicrobial peptide database as a tool for research and education. *Nucleic Acids Res* **2016,** *44* (D1), D1087-D1093.

5. Starr, C. G.; Ghimire, J.; Guha, S.; Hoffmann, J. P.; Wang, Y.; Sun, L.; Landreneau, B. N.; Kolansky, Z. D.; Kilanowski-Doroh, I. M.; Sammarco, M. C.; Morici, L. A.; Wimley, W. C., Synthetic molecular evolution of host cell-compatible, antimicrobial peptides effective against drug-resistant, biofilm-forming bacteria. *Proc Natl Acad Sci U S A* **2020,** *117* (15), 8437-8448.

6. Starr, C. G.; Wimley, W. C., Antimicrobial peptides are degraded by the cytosolic proteases of human erythrocytes. *Biochim. Biophys Acta* **2017,** *1859* (12), 2319-2326.

7. Starr, C. G.; He, J.; Wimley, W. C., Host Cell Interactions Are a Significant Barrier to the Clinical Utility of Peptide Antibiotics. *ACS Chem. Biol* **2016,** *11* (12), 3391-3399.

8. Wimley, W. C., Describing the mechanism of antimicrobial peptide action with the interfacial activity model. *ACS Chem. Biol* **2010,** *5* (10), 905-917.

9. Rathinakumar, R.; Walkenhorst, W. F.; Wimley, W. C., Broad-spectrum antimicrobial peptides by rational combinatorial design and high-throughput screening: The importance of interfacial activity. *J. Am. Chem. Soc* **2009,** *131*, 7609-7617.

10. Rathinakumar, R.; Wimley, W. C., Biomolecular engineering by combinatorial design and high-throughput screening: small, soluble peptides that permeabilize membranes. *J. Am. Chem. Soc* **2008,** *130* (30), 9849-9858.

11. Rathinakumar, R.; Wimley, W. C., High-throughput discovery of broad-spectrum peptide antibiotics. *FASEB J* **2010,** *24*, 3232-3238.

12. Chen, K.; McAleer, J. P.; Lin, Y.; Paterson, D. L.; Zheng, M.; Alcorn, J. F.; Weaver, C. T.; Kolls, J. K., Th17 cells mediate clade-specific, serotype-independent mucosal immunity. *Immunity* **2011,** *35* (6), 997-1009.

13. Marsh, J. W.; Mustapha, M. M.; Griffith, M. P.; Evans, D. R.; Ezeonwuka, C.; Pasculle, A. W.; Shutt, K. A.; Sundermann, A.; Ayres, A. M.; Shields, R. K.; Babiker, A.; Cooper, V. S.; Van Tyne, D.; Harrison, L. H., Evolution of Outbreak-Causing Carbapenem-Resistant Klebsiella pneumoniae ST258 at a Tertiary Care Hospital over 8 Years. *mBio* **2019,** *10* (5).

14. Conlan, S.; Thomas, P. J.; Deming, C.; Park, M.; Lau, A. F.; Dekker, J. P.; Snitkin, E. S.; Clark, T. A.; Luong, K.; Song, Y.; Tsai, Y. C.; Boitano, M.; Dayal, J.; Brooks, S. Y.; Schmidt, B.; Young, A. C.; Thomas, J. W.; Bouffard, G. G.; Blakesley, R. W.; Program, N. C. S.; Mullikin, J. C.; Korlach, J.; Henderson, D. K.; Frank, K. M.; Palmore, T. N.; Segre, J. A., Single-molecule sequencing to track plasmid diversity of hospital-associated carbapenemase-producing Enterobacteriaceae. *Sci Transl Med* **2014,** *6* (254), 254ra126.

15. Snitkin, E. S.; Zelazny, A. M.; Thomas, P. J.; Stock, F.; Henderson, D. K.; Palmore, T. N.; Segre, J. A., Tracking a Hospital Outbreak of Carbapenem-Resistant Klebsiella pneumoniae with Whole-Genome Sequencing. *Sci. Transl. Med* **2012,** *4* (148), 148ra116.

16. Soldano, A.; Yao, H.; Punchi Hewage, A. N. D.; Meraz, K.; Annor-Gyamfi, J. K.; Bunce, R. A.; Battaile, K. P.; Lovell, S.; Rivera, M., Small Molecule Inhibitors of the Bacterioferritin (BfrB)-Ferredoxin (Bfd) Complex Kill Biofilm-Embedded Pseudomonas aeruginosa Cells. *ACS Infect Dis* **2021,** *7* (1), 123-140.

17. Soldano, A.; Yao, H.; Chandler, J. R.; Rivera, M., Inhibiting Iron Mobilization from Bacterioferritin in Pseudomonas aeruginosa Impairs Biofilm Formation Irrespective of Environmental Iron Availability. *ACS Infect Dis* **2020,** *6* (3), 447-458.

18. Clark, J.; Maaloe, O., DNA Replication and the Division Cycle in Escherichia coli. *J Mol Biol* **1967,** *23*, 99-103.

19. Andrews, J. M., Determination of minimum inhibitory concentrations. *J Antimicrob Chemother* **2001,** *48 Suppl 1*, 5-16.

20. Vorregaard, M. Comstat2 - a modern 3D image analysis environment for biofilms. Technical University of Denmark, 2008.

21. Heydorn, A.; Nielsen, A. T.; Hentzer, M.; Sternberg, C.; Givskov, M.; Ersboll, B. K.; Molin, S., Quantification of biofilm structures by the novel computer program COMSTAT. *Microbiology* **2000,** *146 (Pt 10)*, 2395-2407.

22. Otsu, N., A Threshold Selection Method for Gray-Level Histograms. *IEEE Transactions on Systems, Man, and Cybernetics* **1979,** *9*, 62-66.

23. Nguyen, L. T.; Chau, J. K.; Perry, N. A.; de, B. L.; Zaat, S. A.; Vogel, H. J., Serum stabilities of short tryptophan- and arginine-rich antimicrobial peptide analogs. *PLoS. One* **2010,** *5* (9).

24. Control, C. F. D. ANTIBIOTIC RESISTANCE THREATS in the United States, 2019 *https://www.cdc.gov/drugresistance/biggest-threats.html* [Online], 2019. http://www.cdc.gov/drugresistance/pdf/ar-threats-2013-508.pdf.

25. Leung, L. M.; Cooper, V. S.; Rasko, D. A.; Guo, Q.; Pacey, M. P.; McElheny, C. L.; Mettus, R. T.; Yoon, S. H.; Goodlett, D. R.; Ernst, R. K.; Doi, Y., Structural modification of LPS in colistin-resistant, KPC-producing Klebsiella pneumoniae. *J Antimicrob Chemother* **2017,** *72* (11), 3035-3042.

26. Ghimire, J.; Guha, S.; Nelson, B. J.; Morici, L. A.; Wimley, W. C., The Remarkable Innate Resistance of Burkholderia bacteria to Cationic Antimicrobial Peptides: Insights into the Mechanism of AMP Resistance. *J Membr Biol* **2022,** *255* (4-5), 503-511.

27. Boucher, H. W.; Talbot, G. H.; Bradley, J. S.; Edwards, J. E.; Gilbert, D.; Rice, L. B.; Scheld, M.; Spellberg, B.; Bartlett, J., Bad bugs, no drugs: no ESKAPE! An update from the Infectious Diseases Society of America. *Clin. Infect. Dis* **2009,** *48* (1), 1-12.

28. Hoffmann, J. P.; Friedman, J. K.; Wang, Y.; McLachlan, J. B.; Sammarco, M. C.; Morici, L. A.; Roy, C. J., In situ treatment with novel microbicide inhibits methicillin resistant Staphylococcus aureus in a murine wound infection model. *Frontiers in Microbiology* **2020,** *10*.

29. Research, G. V., Diabetic Foot Ulcer Treatment Market Size Worth $6.82 Billion By 2025. 2019; pp https://www.grandviewresearch.com/press-release/global-diabetic-foot-ulcer-dfu-treatment-market.

30. Buch, P. J.; Chai, Y.; Goluch, E. D., Treating Polymicrobial Infections in Chronic Diabetic Wounds. *Clin Microbiol Rev* **2019,** *32* (2).

31. Ramirez-Acuna, J. M.; Cardenas-Cadena, S. A.; Marquez-Salas, P. A.; Garza-Veloz, I.; Perez-Favila, A.; Cid-Baez, M. A.; Flores-Morales, V.; Martinez-Fierro, M. L., Diabetic Foot Ulcers: Current Advances in Antimicrobial Therapies and Emerging Treatments. *Antibiotics (Basel)* **2019,** *8* (4).

32. Rice, J. B.; Desai, U.; Cummings, A. K.; Birnbaum, H. G.; Skornicki, M.; Parsons, N. B., Burden of diabetic foot ulcers for medicare and private insurers. *Diabetes Care* **2014,** *37* (3), 651-8.

33. Saltoglu, N.; Ergonul, O.; Tulek, N.; Yemisen, M.; Kadanali, A.; Karagoz, G.; Batirel, A.; Ak, O.; Sonmezer, C.; Eraksoy, H.; Cagatay, A.; Surme, S.; Nemli, S. A.; Demirdal, T.; Coskun, O.; Ozturk, D.; Ceran, N.; Pehlivanoglu, F.; Sengoz, G.; Aslan, T.; Akkoyunlu, Y.; Oncul, O.; Ay, H.; Mulazimoglu, L.; Erturk, B.; Yilmaz, F.; Yoruk, G.; Uzun, N.; Simsek, F.; Yildirmak, T.; Yasar, K. K.; Sonmezoglu, M.; Kucukardali, Y.; Tuna, N.; Karabay, O.; Ozgunes, N.; Sargin, F.; Turkish Society of Clinical, M.; Infectious Diseases, D. F. I. S. G., Influence of multidrug resistant organisms on the outcome of diabetic foot infection. *Int J Infect Dis* **2018,** *70*, 10-14.

34. Richard, J. L.; Sotto, A.; Lavigne, J. P., New insights in diabetic foot infection. *World J Diabetes* **2011,** *2* (2), 24-32.

35. Shai, Y., Mode of action of membrane active antimicrobial peptides. *Biopolymers* **2002,** *66* (4), 236-248.

36. Shai, Y.; Oren, Z., From "carpet" mechanism to de-novo designed diastereomeric cell-selective antimicrobial peptides. *Peptides* **2001,** *22* (10), 1629-1641.

37. Guha, S.; Ghimire, J.; Wu, E.; Wimley, W. C., Mechanistic Landscape of Membrane-Permeabilizing Peptides. *Chem. Rev* **2019,** *119*, 6040-6085.

38. Khanolkar, R. A.; Clark, S. T.; Wang, P. W.; Hwang, D. M.; Yau, Y. C. W.; Waters, V. J.; Guttman, D. S., Ecological Succession of Polymicrobial Communities in the Cystic Fibrosis Airways. *mSystems* **2020,** *5* (6).

39. Gloag, E. S.; Marshall, C. W.; Snyder, D.; Lewin, G. R.; Harris, J. S.; Santos-Lopez, A.; Chaney, S. B.; Whiteley, M.; Cooper, V. S.; Wozniak, D. J., Pseudomonas aeruginosa Interstrain Dynamics and Selection of Hyperbiofilm Mutants during a Chronic Infection. *mBio* **2019,** *10* (4).

40. Moradali, M. F.; Ghods, S.; Rehm, B. H., Pseudomonas aeruginosa Lifestyle: A Paradigm for Adaptation, Survival, and Persistence. *Front Cell Infect. Microbiol* **2017,** *7*, 39.

41. Fernandez, L.; Alvarez-Ortega, C.; Wiegand, I.; Olivares, J.; Kocincova, D.; Lam, J. S.; Martinez, J. L.; Hancock, R. E., Characterization of the polymyxin B resistome of Pseudomonas aeruginosa. *Antimicrob Agents Chemother* **2013,** *57* (1), 110-9.

42. Esani, S.; Chen, T.; Leung, K. P.; Van Laar, T. A., Transcriptome Sequence of Antibiotic-Treated Pseudomonas aeruginosa. *Microbiol Resour Announc* **2019,** *8* (12).

43. Hancock, R. E., Resistance mechanisms in Pseudomonas aeruginosa and other nonfermentative gram-negative bacteria. *Clin. Infect. Dis* **1998,** *27 Suppl 1*, S93-S99.

44. Lazar, V.; Martins, A.; Spohn, R.; Daruka, L.; Grezal, G.; Fekete, G.; Szamel, M.; Jangir, P. K.; Kintses, B.; Csorgo, B.; Nyerges, A.; Gyorkei, A.; Kincses, A.; Der, A.; Walter, F. R.; Deli, M. A.; Urban, E.; Hegedus, Z.; Olajos, G.; Mehi, O.; Balint, B.; Nagy, I.; Martinek, T. A.; Papp, B.; Pal, C., Antibiotic-resistant bacteria show widespread collateral sensitivity to antimicrobial peptides. *Nat Microbiol* **2018,** *3* (6), 718-731.